COMMUNICATIONS

DE LA FACULTÉ DES SCIENCES
DE L'UNIVERSITÉ D'ANKARA

Série B Chimie

TOME : 28 ANNEE : 1982

Formation Characteristics of Cuprous Oxide

by

Gözen BEREKET and Melike KABASAKALOĞLU*

6

Faculté des Sciences de l'Université d'Ankara
Ankara, Turquie

Communications de la Faculté des Sciences de l'Université d'Ankara

Comité de Redaction de la Série B
E. Alper, S. Gümüş, T. Gündüz, Y. Sarıkaya, C. Tüzün
Secrétaire de Publication
Ö. Çakar.

La Revue "Communications de la Faculté des Sciences de l'Université d'Ankara" est un organe de publication englobant toutes les diciplines scientifique représentées à la Faculté des Sciences de l'Université d'Ankara.

La Revue, jusqu'à 1975 à l'exception des tomes I, II, III etait composé de trois séries

Série A: Mathématiques, Physique et Astronomie,
Série B: Chimie,
Série C: Sciences Naturelles.

A partir de 1975 la Revue comprend sept séries:

Série A_1: Mathématiques,
Série A_2: Physique,
Série A_3: Astronomie,
Série B: Chimie,
Série C_1: Géologie,
Série C_2: Botanique,
Série C_3: Zoologie.

En principe, la Revue est réservée aux mémoires originaux des membres de la Faculté des Sciences de l'Université d'Ankara. Elle accepte cependant, dans la mesure de la place disponible les communications des auteurs étrangers. Les langues Allemande, Anglaise et Française seront acceptées indifféremment. Tout article doit être accompagnés d'un resume.

Les articles soumis pour publications doivent être remis en trois exemplaires dactylographiés et ne pas dépasser 25 pages des Communications, les dessins et figures portes sur les feuilles séparées devant pouvoir être reproduits sans modifications.

Les auteurs reçoivent 25 extraits sans couverture.

l'Adresse : Dergi Yayın Sekreteri,
Ankara Üniversitesi,
Fen Fakültesi,
Beşevler-Ankara

Formation Characteristics of Cuprous Oxide

Gözen BEREKET and Melike KABASAKALOĞLU*

Department of Chemistry Faculty of Science. University of Ankara/TURKEY

(Received May 17, 1982; accepted June 18, 1982)

ABSTRACT

Formation and growth mechanism of Cu_2O films in 1 N NaOH solution were investigated. Two different Cu_2O films were grown on the copper surface depending on time. Growth of the first film is rapid. The growth of the second one is slow. The second film is formed from the precipitation of copper (1) ions. The growth rate of these films are in accordance with the parabolic growth law.

INTRODUCTION

Formation of different Cu_2O films by dissolution-precipitation mechanism during anodic oxidation of copper in 1 N NaOH were postulated previously [1]. In this study formation and growth mechanism of Cu_2O films were investigated.

Formation of passivating films in aqueous solutions were extensively studied and growth models were demonstrated [2]. For low fields or thick films, assuming a) region of space charge at the two interfaces can be neglected and b) the rate of growth is controlled by the rate of diffusion of metal ions across the oxide layer, the rate of growth can be written as

$$\frac{dx}{dt} = \frac{4a^2\ n\upsilon\ q\ V\ \Omega}{k\ T\ x} \exp\left[-\frac{U}{kT}\right] \qquad (1)$$

Where a is the half-jump distance for the ions, υ and n are the vibration frequency and the concentration of ions at x respectively. V is the po-

* Present adress, Ankara Üniversitesi, Fen Fakültesi Kimya Bölümü Ankara TURKEY.

tential across the film of thickness x. Ω is the volume of oxide per metal ion and t is the time.

Defining

$$K_p = \frac{4\ a^2\ n\ \upsilon\ q\ V\ \Omega}{k\ T} \exp\left[-\frac{U}{kT}\right] \tag{2}$$

and by integration

$$X^2 = 2\ K_p t + C \tag{3}$$

is obtained. For t=O, x=O and C=O is obtained. Parabolic growth law is found as

$$X^2 = 2\ K_p t \tag{4}$$

EXPERIMENTAL

Electrolitic cell, electrodes, potentiostat and recorder system were the same as previous study [1]. For the system obeying dissolution-precipitation mechanism, cathodic sweeps are severely depended on the anodic scan limit potentials and on the oxidation time at these potentials. In the present study, the electrode was first oxidized by linear sweep to different anodic potentials at 50 mV/sec and waited for different period of time without current interruption at these anodic potentials and then, potential sweep was reversed. The reverse scans were also obtained at the same sweep rate of 50 mV/sec. The potentials in figures are against saturated calomel electrode.

RESULT

Figures (1–8) show the curves obtained by the described way in the previous paragraph. Initial potential was-1200 mV. The oxidation times at different scan limit potentials (Eλ) were shown on the curves. For Eλ < –545 mV no matter how long the electrode is oxidized at Eλ, no peak was obtained indicating the reduction of the oxidation product of the metal or oxide film (Fig. 1). The volume of the test solution was about 150 cc. and it was greater than the area of the electrode (0,06 cm^2). So the effect of soluble species on the reduction peaks of oxide films formed by anodic polarization can be neglected. The peaks or

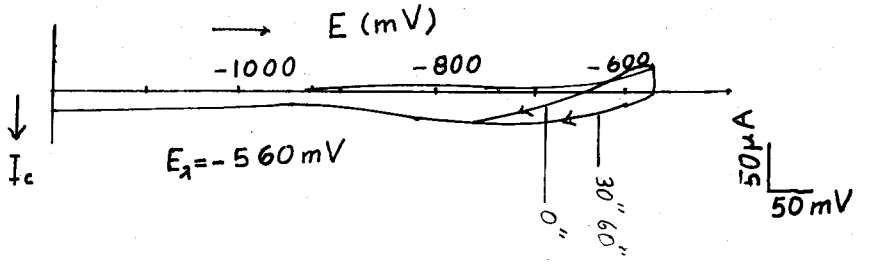

Fig 1. Current-potential curves obtained by cyclic voltammetry. Sweep rate was 50 mV/sec. The potential of the electrode hold at –560 mV for 0, 30 and 60 seconds before potential reversal.

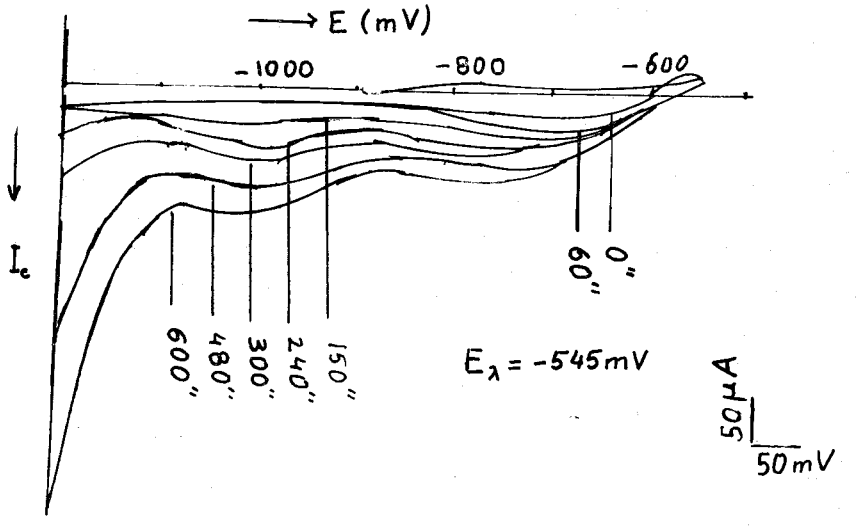

Fig 2. Current-potential curves obtained by cyclic voltammetry. Sweep rate was 50 mV/sec. The potential of the electrode hold at –545 mV for different period of time (0–600") before potential reversal.

steps on the reduction curves were attributed to the reduction of oxide films or reduction of soluble species in the pores of the oxide that could not diffuse away into solution.

For $E\lambda = -545$ mV (Fig. 2) cathodic polarization curve obtained without waiting at $E\lambda$ has weakly pronounced peak at –700 mV [peak (I)] is obtained. But, if the oxidation time at $E\lambda$ is increased, the current at –700 mV is increased and also the second peak [peak (II)] at –1000 mV and the potential step at –1100 mV appeared after certain period of oxidation time in the cathodic region.

The curves in Fig. (3–8) obtained for different $E\lambda$ values by the same way as in Fig. (1–2) show that the first peak always appears whatever the oxidation time at $E\lambda$ is and its peak potential shifts to –800 mV by oxidation time at $E\lambda$. The appearance time of the second peak and the third step at –1100 mV on the cathodic curves depend on the anodic scan limit potentials and the oxidation time at these values. The second peak appears at –1000 mV after the oxidation for 20 or 30 second and its peak current increases by oxidation time.

The appearance time of the third step at –1100 mV is longer than the appearance time of the second step. For instance, the third step is observed after the oxidation for 150 seconds at $E\lambda = -545$ mV and for $E\lambda = -530$ mV the appearance of it requires oxidation for 100 seconds. Third step is disappeared for $E\lambda > -515$ mV.

DISCUSSION

The beginning potential of peak (I) is –600 mV and this value is very close to the equilibrium potential of Cu_2O/Cu system with respect to S.C.E. [2]. So this peak was explained by the reduction of Cu_2O to Cu. We proposed [1] the following reaction mechanism for the formation of Cu_2O

$$Cu + n\ OH^- \rightarrow Cu(OH)_n^{1-n} + e^- \quad (5)$$

$$2Cu + 2OH^- \rightarrow (Cu_2O)_I + H_2O + 2e^- \quad (6)$$

$$2Cu\ (OH)_n^{1-n} \rightarrow (Cu_2O)_{II} + (2n—2)\ OH^- + H_2O \quad (7)$$

Because, the first film has a porous nature and sweep rate is high, $Cu(OH)_n^{1-n}$ ions can be diffuse away into solution from the electrode sur-

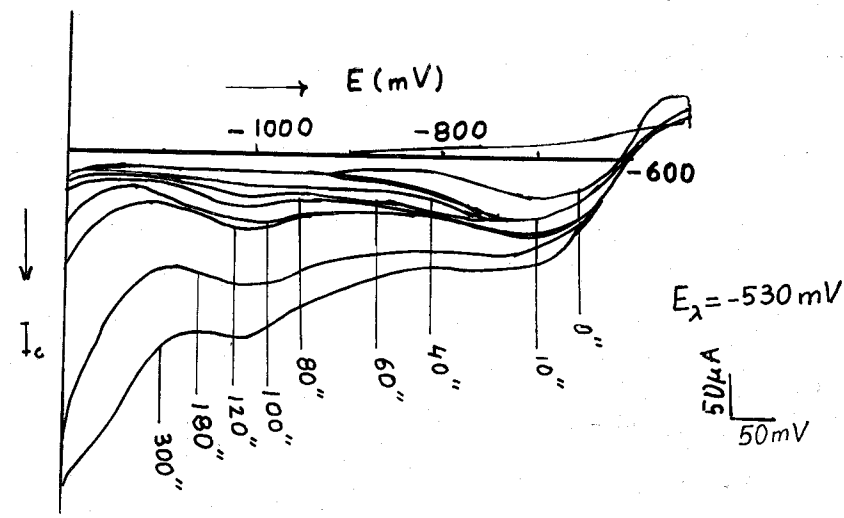

Fig 3. Current-potential curves obtained by cyclic voltammetry. Sweep rate was 50 mV/sec. The potential of the electrode hold at -530 mV for different period of time (0–300") before potential reversal.

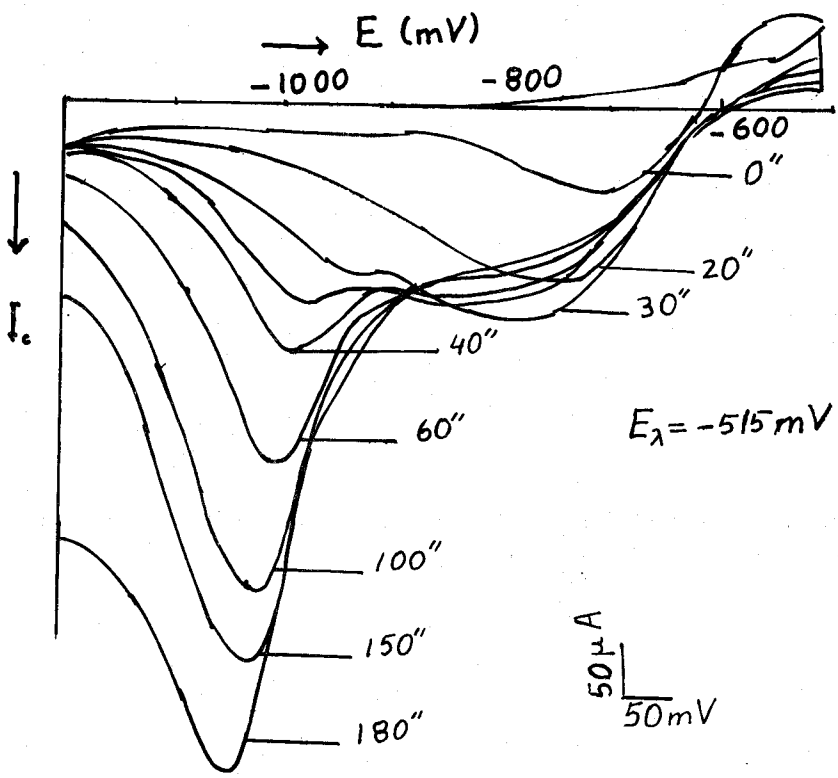

Fig 4. Current-potantial curves obtained by cyclic voltammetry. Sweep rate was 50 mV/sec. The potential of the electrode hold at -515 mV for different period of time (0–180") before potential reversal.

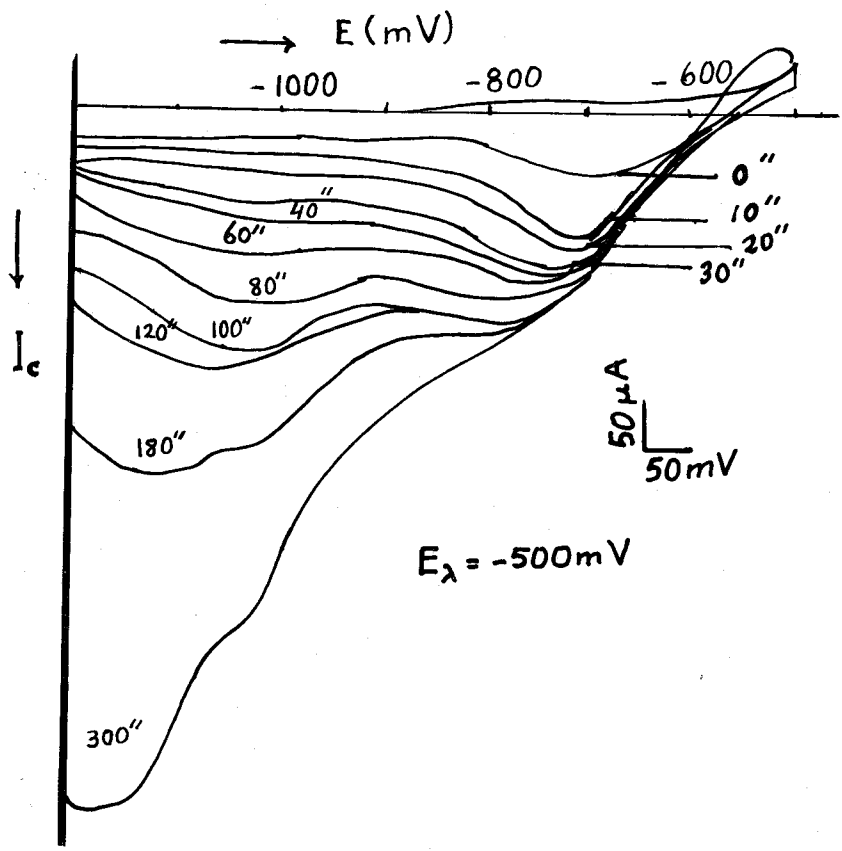

Fig 5. Current-potential curves obtained by cyclic voltammetry. Sweep rate was 50 mV/sec. The potential of the electrode hold at -500 mV for different period of time (0–300") before potential reversal.

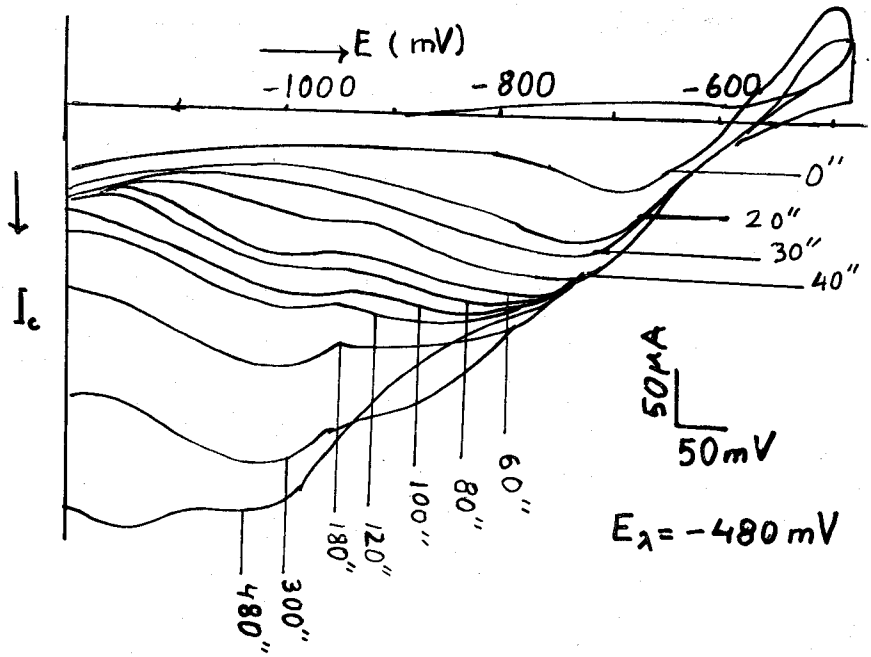

Fig 6. Current-potential curves obtained by cyclic voltammetry. Sweep rate was 50 mV/sec. The potential of the electrode hold at –480 mV for different period of time (0–480") before potential reversal.

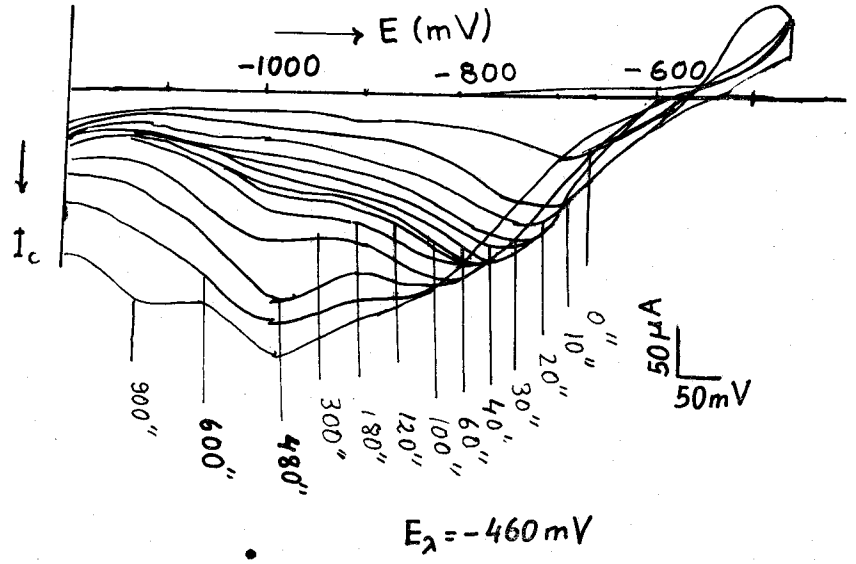

Fig 7. Current-potential curves obtained by cyclic voltammetry. Sweep rate was 50 mV/sec. The potential of the electrode hold at –460 mV for different period of time (0–900") before potential reversal.

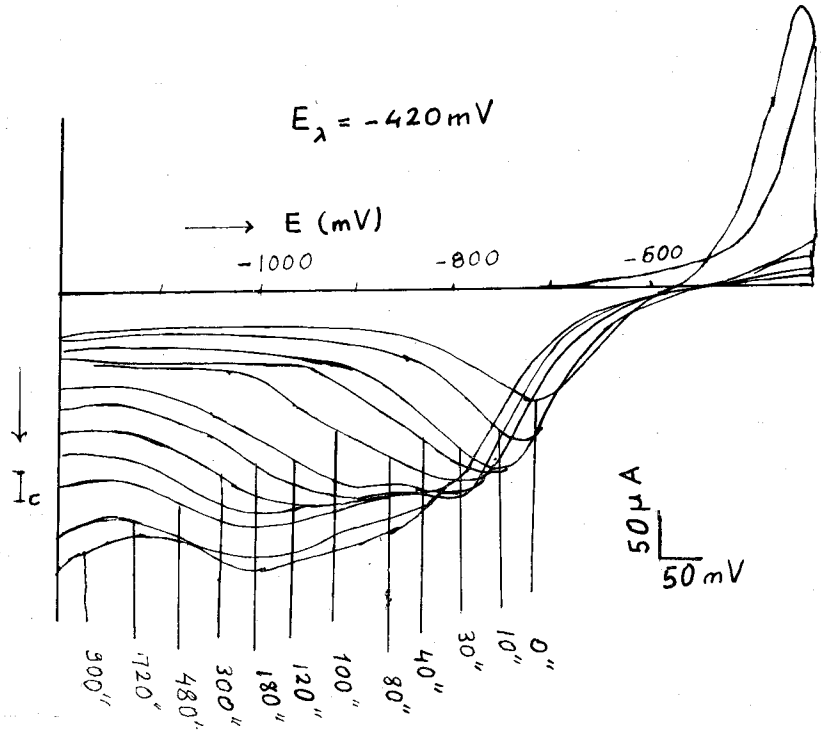

Fig 8. Current-potential curves obtained by cyclic voltammetry. Sweep rate was 50 mV/sec. The potential of the electrode hold at −420 mV for different period of time (0–900") before potential reversal.

face and only one cathodic peak associated with the reduction of $(Cu_2O)_I$ film at –700 mV is observed on the reduction voltammograms. If the oxidation time at Eλ is increased the amount of the first film and the soluble anion, $Cu(OH)_n^{1-n}$ are also increased. Reactions (5–7) have the opportunity to take place. For the formation of the second film, first $(Cu_2O)_I$ acts as crystalization nuclea. So the second $(Cu_2O)_{II}$ film has different formation free energy and structure than the first $(Cu_2O)_I$ film, the second $(Cu_2O)_{II}$ reduces at different potential from the first one.

At lower potentials, electrode surface is not completely covered by the films. Soluble $Cu(OH)_n^{1-n}$ ions formed by anodic polarization form the second $(Cu_2O)_{II}$ film on the first $(Cu_2O)_I$ film which has been previously formed by reaction (6) on the surface. Some of these soluble ions diffuse away into solution and some of them remain in the pores of the first and the second film. Soluble ions remain in the pores of the films are reduced at –1100 mV. As the anodic scan limit, Eλ is increased the amount of the first film $(Cu_2O)_I$ is increased by reaction (6) and the amount of second film $(Cu_2O)_{II}$ is also increased associated with the increment of the amount of first film.

For higher potentials, surface is covered by these films at appreciable degree and the rate of reaction (5) is decreased. As a result the concentration of $Cu(OH)_n^{1-n}$ anions on the surface is decreased and the step at –1100 mV is disappeared.

The areas under the curves in figures (2–8) are proportional with the amount of charge passed at cathodic region. Total cathodic charges per surface area of the electrode, Q total (mC/cm²), were calculated from the curves and shown in table I as a function of time and anodic scan limit potentials (Eλ). In this table Q_I denotes the charge between –600 mV and –900 mV i.e. the domain of the first peak and can be taken as the reduction of the first $(Cu_2O)_I$ film. $(Q_{total} - Q_I)$ shows the charge between –900 mV and –1200 mV and can be taken approximately as the reduction charge of the second $(Cu_2O)_{II}$ film for $E\lambda > -515$ mV. The first line in table I shows the reduction charges $(Q_{t=o})$ associated to the double layer and the reduction of the (Cu_2O) films formed during anodic sweep to various Eλ values at 50 mV/sec.

In order to find the variation of charges belong to the growth of the first and second film which formed during holding period of the

TABLE I

Cathodic Charges Calculated from Figures (2–9).

E λ		−545mV			−530mV			−515mV			−500mV			−480mV			−460mV			−420mV		
t sec.	$\sqrt{t}$ Sec.$^{\frac{1}{2}}$	Q values as mC/cm²																				
		Q_T	Q_I	Q_T-Q_I	Q_T	Q_I	Q_T-Q_I	Q_T	Q_I	Q_T-Q_I	Q_T	Q_I	Q_T-Q_I	Q_T	Q_I	Q_T-Q_I	Q_T	Q_I	Q_T-Q_I	Q_T	Q_I	Q_T-Q_I
0	0	1.79	0.79	1	2.29	1.29	1.0	3.41	2.16	1.25	7.33	3.75	3.58	8.75	4.16	4.83	7.17	4.66	2.51	11.33	6.67	4.66
10	3.16	2.62	1.04	1.25	4.04	2.79	1.25	7.29	5.08	2.20	11.92	6.67	5.25	13.08	7.92	6.067	12.67	8.50	4.17	15.67	10.00	5.67
20	4.47	1.79	0.54	1.25*	3.75	2.5	1.25*	9.92	6.29	3.63*	14.17	8.33	5.83*	15.67	8.17	7.50*	12.83	7.83	4.83	16.67	11.25	5.42
30	5.47	2.4	1.12	1.25	2.75	2.79	2.28	–	–	–	16.67	9.38	7.29	17.33	10.17	7.17	15.00	9.66	5.33	18.18	11.67	6.50
40	6.32	1.42	0.16	1.25	4.04	2.29	1.75	12.5	6.67	5.83	21.5	11.08	11.42	19.67	10.92	8.75	16.25	10.42	5.83	21.42	13.33	8.08
60	7.74	2.38	1.12	1.25	5.0	2.29	2.7	16.25	6.67	9.58	26.42	12.50	13.92	23.67	12.50	11.16	17.67	11.42	6.25	22.50	13.33	9.17
80	8.94	3.08	1.79	1.25	5.83	2.15	3.08	18.58	6.58	12.0	26.67	12.75	13.92	24.42	12.50	11.92	19.17	11.33	7.84	25.00	13.75	12.08
100	10	–	–	–	5.83	–	3.17	19.17	6.25	12.92	29.53	13.33	16.25	26.67	12.83	13.83	20.00	11.83	8.17	27.50	11.25	16.25
120	10.95	3.13	1.88	1.25	4.54	2.79	4.04	22.08	6.5	15.58	35.67	13.33	28.33	28.33	15.00	13.33	20.58	12.17	8.42	29.83	12.50	17.33
180	13.41	4.04	2.08	1.96	12.5	3.12	9.38	26.67	6.25	20.42	45.83	13.33	32.50	35.25	15.17	20.03	23.33	13.17	10.17	32.50	12.50	20.00
240	15.49	4.92	2.13	2.79	–	–	–	–	–	–	–	–	–	–	–	–	–	–	–	–	–	–
300	17.32	6.25	2.5	3.75	21.83	3.62	18.2	–	–	–	62.33	15.00	47.33	43.49	15.17	28.33	26.67	13.17	13.50	33.75	12.08	21.66
480	21.9	9.5	3.63	5.88	–	–	–	–	–	–	–	–	–	47.50	16.67	30.83	28.5	13.33	15.17	34.75	12.083	22.67
600	24.49	11.46	3.98	8.38	–	–	–	–	–	–	–	–	–	–	–	–	32.17	13.16	19.00	–	–	–
720	26.83	–	–	–	–	–	–	–	–	–	–	–	–	–	–	–	–	–	–	38.33	16.00	25.00
900	30	–	–	–	–	–	–	–	–	–	–	–	–	–	–	–	35.83	14.00	21.83	40.83	16.00	27.50

* These values are taken as the Q_{II} (t=O) in plotting fig 14. The Q values in the first line are used for correction in plotting fig 9–11.

electrode potential at Eλ, correction was made for each Eλ value by substracting $Q_{t=o}$ value from corresponding Q_t values, Fig. 9.10 and 11 show the variation of corrected Q_{total}, Q_I and $Q_T - Q_I$ values with time. For Eλ = –545 mV and –530 mV Q_{total} v.s.t and $(Q_{total} - Q_I)$ v.s.t curves have two steps. The second step in these curves is due to the third step at –1100 mV in Fig. (2–3).

In Fig. 10, dotted curves show the variation of Q_I values corrected for only double layer charge. In the potential region of the first peak the calculated cathodic charge (0.8 mC/cm²) from the curve in Fig. 1 was taken as the double layer charge. The charge associated to the first peak increases with Eλ. For Eλ ≥ –500 mV Q_I becomes constant around 12 mC/cm². The film thickness, x, associated with this charge assuming roughness factor as r = 3.7 [4] and using Faraday Law,

$$x = \frac{Q \cdot M}{\rho \, z \, Fr} \tag{8}$$

where Q (12.10^{-3} C/cm²) is the cathodic charge per surface area of the electrode, M (143 gr/mole.) and ρ (6 gr/cm³) are the molecular weight and density of Cu_2O respectively. Z and F are the known values

$$x = \frac{12.10^{-3} \cdot 143}{6.2.96500.3.7} = 4.10^{-7} \text{ cm} \tag{9}$$

was found. Remembering that thickness of monomolecular oxide layer was equal to 3–4 10^{-8} cm [5, 6], the first $(Cu_2O)_1$ film is found to grow no thicker than ten molecular layers.

From the above formula thickness x is proportional with charge Q. For this reason using Q instead of x, we can find out if growth of the films obey parabolic growth law The corrected Q_I and $(Q_{total} - Q_I)$ values whose variation shown in figures 10–11 were plotted against square root of time in figures 12 and 13. All curves in fig. 12 are linear passing through origin and the film reduced at peak I obeys parabolic growth law.

In fig 13 $(Q_{total} - Q_I)$ v.s $\sqrt{t}$ is linear but lines do not pass through origin for Eλ = –515 mV, –530 mV, –500 mV and –480 mV. Extrapolating these lines for $(Q_T - Q_I) = O$, all lines cut each other at $t = 4.47 = \sqrt{20}$ $(sec.)^{1/2}$ value. For Eλ = –460 mV $(Q_T - Q_I)$ v.s $\sqrt{t}$ is linear passing through origin.

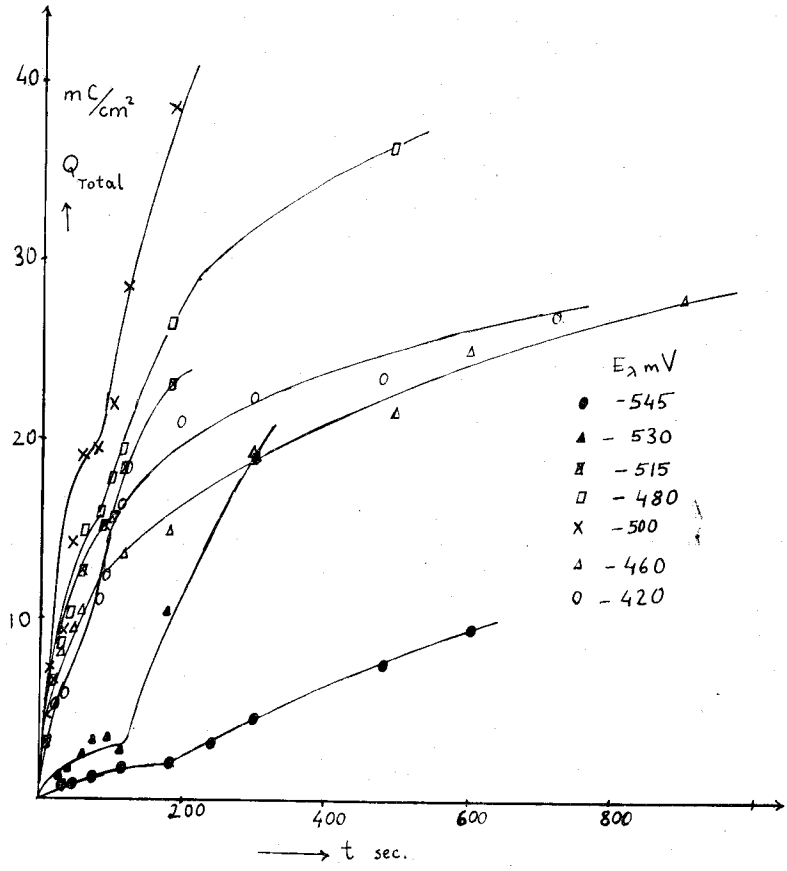

Fig 9. The variation of total cathodic charge with time.

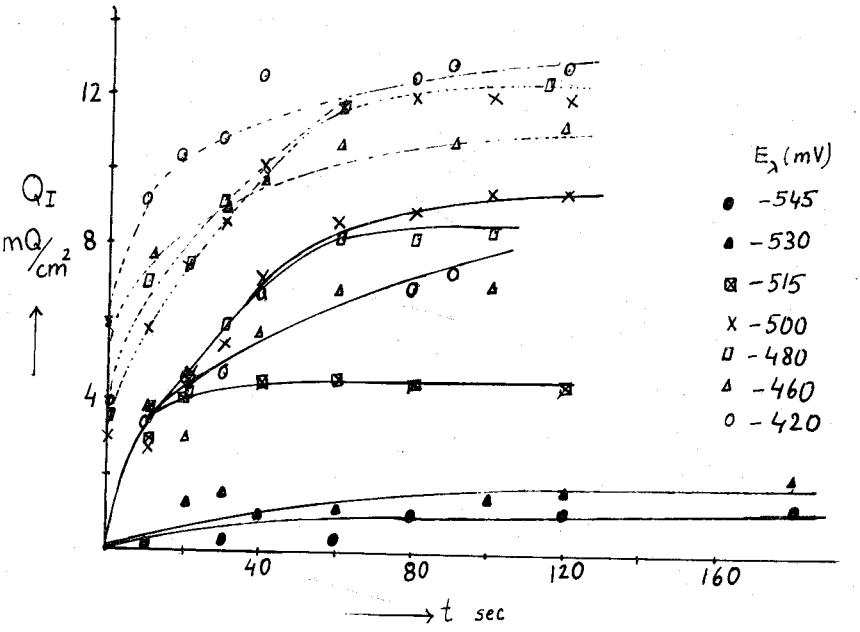

Fig 10. The variation of the charge associated to the first peak with oxidation period.

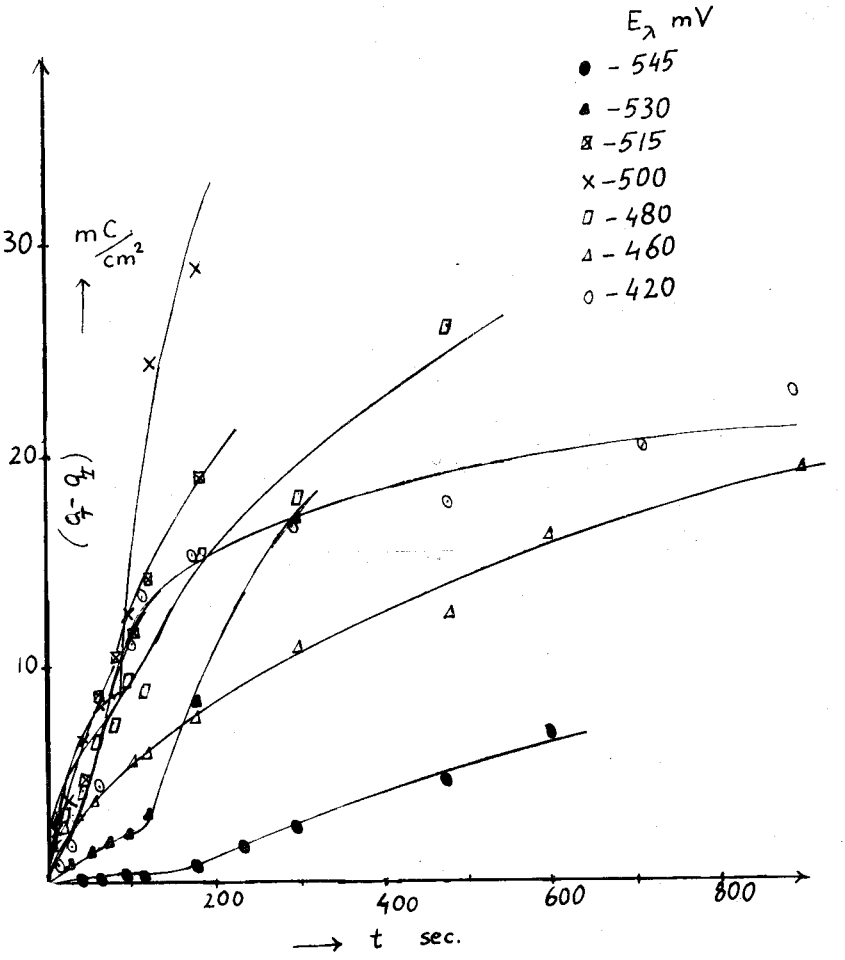

Fig 11. The variation of the charge associated to the second peak with oxidation period.

This indicates that only the first film is formed between –530 mV and –480 mV potential range during anodic scan. Period of time keeping electrode at potential range between –515 mV and –480 mV should be twenty seconds, in order that the second film be formed. For $E\lambda = -460$ mV the first and the second films are formed together during anodic scan. So $(Q_T - Q_I)$ v.s. $\sqrt{t}$ is linear and passes through origin.

For the potential range between –900 mV and –1200 mV in Figures (3–6), $(Q_{total} - Q_I)_{t=20}$ values were assumed as $(Q_{II})_{t=o}$ charge, i.e, the double layer charge and the residual charge of the first film, correction were done by substracting each $(Q_{II})_{t=o}$ values from corresponding $(Q_{total} - Q_I)_t$ values for $E\lambda = -530$ mV, –515 mV, –500 mV and –480 mV. These corrected Q_{li} (mC/cm^2) values were plotted v.s. $\sqrt{t-20} = \sqrt{t'}$ in fig.14. These curves are linear passing through origin. These results show that the second film also obeys the parabolic growth law. The slope of the lines in Figures 12 and 14 are proportional with the Kp value in equation (4). These slopes of the lines in Fig.12 increase with $E\lambda$ and stay constant for $E\lambda > -515$ mV. The slopes of lines in Fig. 14 first increase and then decrease with $E\lambda$.

If we take the n value in equation (2) as the concentration of soluble $Cu(OH)_n^{1-n}$ ions in the films the explanation of the change of the slopes of the lines with $E\lambda$ can be possible. Depending on the surface coverage or the thickness of the film the rate of the reaction (5) and then the concentration of soluble $Cu(OH)_n^{1-n}$ changes.

For $E\lambda < -500$ mV, the thickness of the film is not high and then n value and K_p are high. For $E\lambda > -500$ mV, because of the formation of thick film the rate of the reaction (5) is decreased and then the concentration of soluble ions is decreased. So the n value and the slopes of the lines in Fig.14 are decreased.

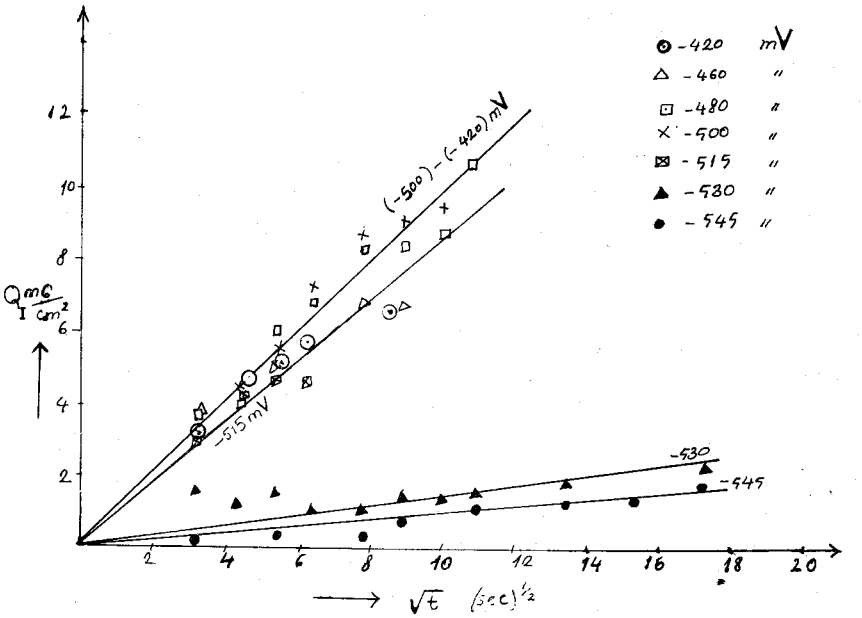

Fig 12. The variation of Q_I with the square root of time. For each $E\lambda$, Q_I values were corrected for corresponding $Q_{t=0}$ value.

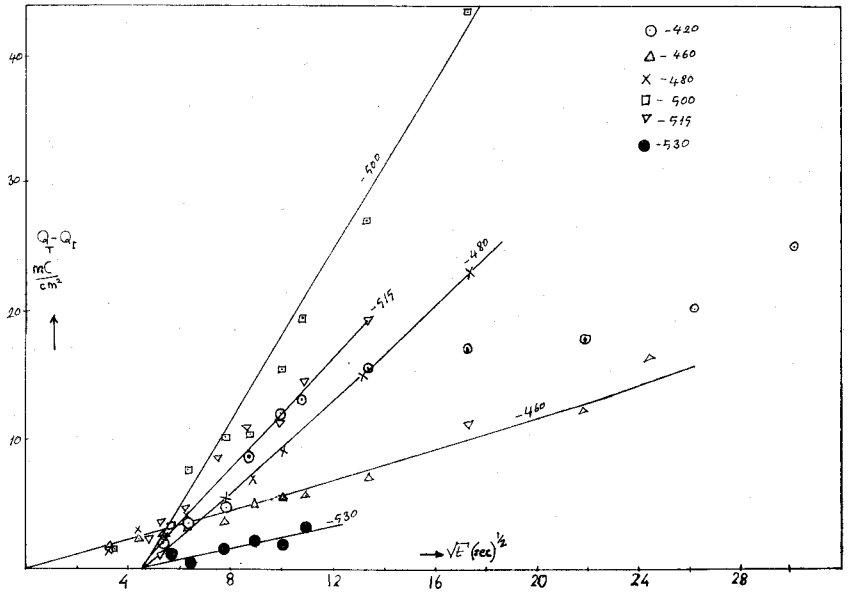

Fig 13. The variation of $Q_{total} - Q_I$ with the square root of time. For each $E\lambda$, $(Q_T - Q_I)$ values were corrected for corresponding $Q_{t=o}$ value.

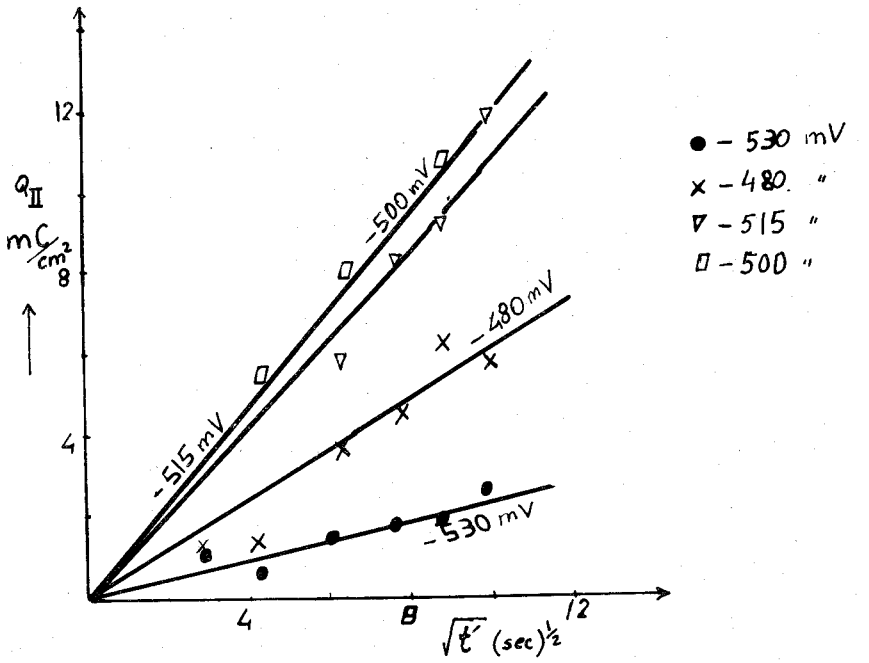

Fig 14. The variation of Q_{II} with the square root of time. For each $E\lambda$, $(Q_T - Q_I)$ values were corrected for corresponding $Q_{t=20}$ value.

REFERENCES

1- **G.Bereket and M.Kabasakaloğlu,** to be Published.

2- **B.E. Conway,** "Theory of Electrode Process" Ronald Press Company Newyork (1962).

3- **M.Pourbaix,** Atlas of Electrochemical Equilibria in Aqueous Solutions, Pergamon Press (1960).

4- **S. Fletcher, R.G. Barradas and D.Porter,** J.Electrochem. Soc. 125, 1960 (1978).

5- **E. Gileadi,** Electrosorption, Plenum press Newyork p. 73 (1967).

6- **D.Dickertmaan, J.W. Schultze and K.J. Vetter,** Electroanal, Chem. 55,429 (1974).

ÖZET

Bu çalışmada 1 N NaOH içinde Cu_2O filmlerinin oluşma ve büyüme mekanizması araştırılmıştır. Zamana bağlı olarak yüzeyde iki farklı Cu_2O filmi büyür. Birinci filmin büyümesi hızlı, ikincinin yavaştır. İkinci film Cu(I) iyonlarından çökme ile olur. Filmler parabolik büyüme kanununa uygun olarak büyürler.